The Effect of Nanoparticle-Enhanced Photoacoustic Stimulation on Multipotent Marrow Stromal Cells

Danielle E. Green,[†] Jon P. Longtin,[‡] and Balaji Sitharaman[†,*]

[†]Department of Biomedical Engineering and [‡]Department of Mechanical Engineering, State University of New York at Stony Brook, Stony Brook, New York 11794-2300

ABSTRACT In this article, we report a novel nanoparticle-enhanced biophysical technique that differentiates multipotent marrow stromal cells (MSCs) toward osteoblasts. We show that a brief (10 min) daily nanoparticle-facilitated exposure of MSCs to nanosecond pulse laser-induced photoacoustic (PA) stimulation enhances their differentiation toward osteoblasts. To observe osteodifferentiation under PA stimulation, tissue culture plates were seeded with MSCs without the osteogenic culture supplements (OS, 0.01 M β-glycerophosphate, 50 mg/L ascorbic acid, 10^{-8} M dexamethasone) in the presence and absence of single-walled carbon nanotubes (SWNTs) and gold nanoparticles (GNPs). The alkaline phosphatase activity, calcium content, and osteopontin secretion were monitored as indicators of MSCs' differentiation toward osteoblasts. The PA stimulated groups show up to 612% increase in calcium content compared to the controls cultured with osteogenic supplements (without PA stimulation) after 16 days. Among the PA stimulated groups, at day 16, MSCs incubated with SWNTs at 10 μg/mL concentrations showed up to 97% greater calcium content than those that did not contain SWNTs. The results demonstrated that PA stimulation not only promotes osteogenesis but also is synergistically enhanced by the presence of nanoparticles and, thus, has major implications for bone regeneration applications.

KEYWORDS: single-walled carbon nanotube · pulse laser · photoacoustic effect · bone regeneration · osteoblast

The phenomenon where absorption of electromagnetic energy generates acoustic waves is known as the photoacoustic (PA) effect. First demonstrated in 1881 by A. G. Bell,[1] this effect is used for a variety of applications in material science and medicine such as imaging and spectroscopy.[2,3] An optical (visible and near-infrared lasers) or radio frequency/microwave source is typically used as the electromagnetic source. This source deposits non-ionizing electromagnetic energy onto an absorbing surface giving rise to a thermoelastic expansion leading to a wide-band ultrasonic emission. This effect forms the basis for emerging bioimaging technologies such as PA microscopy and imaging.[3] Recently, a number of nanomaterials such as single-walled carbon nanotubes (SWNTs) and gold nanoparticles (GNPs) with strong intrinsic absorption at visible/near-infrared (NIR) wavelengths have been used as contrast agents for laser-induced PA imaging.[4−6]

Marrow, or mesenchymal stromal cells (MSCs), are multipotent cells found predominantly within the bone marrow. MSCs are undifferentiated progenitor cells for various mesenchymal tissues and can differentiate into tissue types including but not limited to bone, cartilage, and adipose.[7−9] Thus, they show potential for a variety of biomedical applications for tissue regeneration,[10,11] cell and gene therapy,[12] with a possibility of clinical translation for promising experimental developments.[13] Proper environmental cues are necessary to differentiate MSCs into various tissue types. Laser-induced optical stimulation,[14,15] low-intensity pulsed ultrasound,[16] mechanical signals,[17] fluid shear stresses,[18] and nanomaterials[19] have been demonstrated to influence their differentiation toward osteoblasts. The ultimate goal of all these strategies is to restore and heal bone loss due to trauma or disease. Curiously, the osteoinductive efficacy of PA stimulation which in theory should combine the benefits of optical and acoustic stimulation has not been explored. To the best of our knowledge, there have been no studies examining the interaction of MSCs and nanoparticles that enhance the PA effect under PA stimulation.

In this work, we aimed to combine PA stimulation and nanomaterials to synergize the benefits of optical, mechanical (acoustic) stimulation and nanomaterials on MSCs' differentiation toward osteoblasts. Toward this goal, we investigated the effect of laser-induced photoacoustic stimulation with and without nanoparticle (SWNTs or GNPs) facilitation on the differentiation of MSCs toward osteoblastic lineages in static culture.

*Address correspondence to balaji.sitharaman@stonybrook.edu.

Received for review April 30, 2009 and accepted July 13, 2009.

Published online July 16, 2009.
10.1021/nn900434p CCC: $40.75

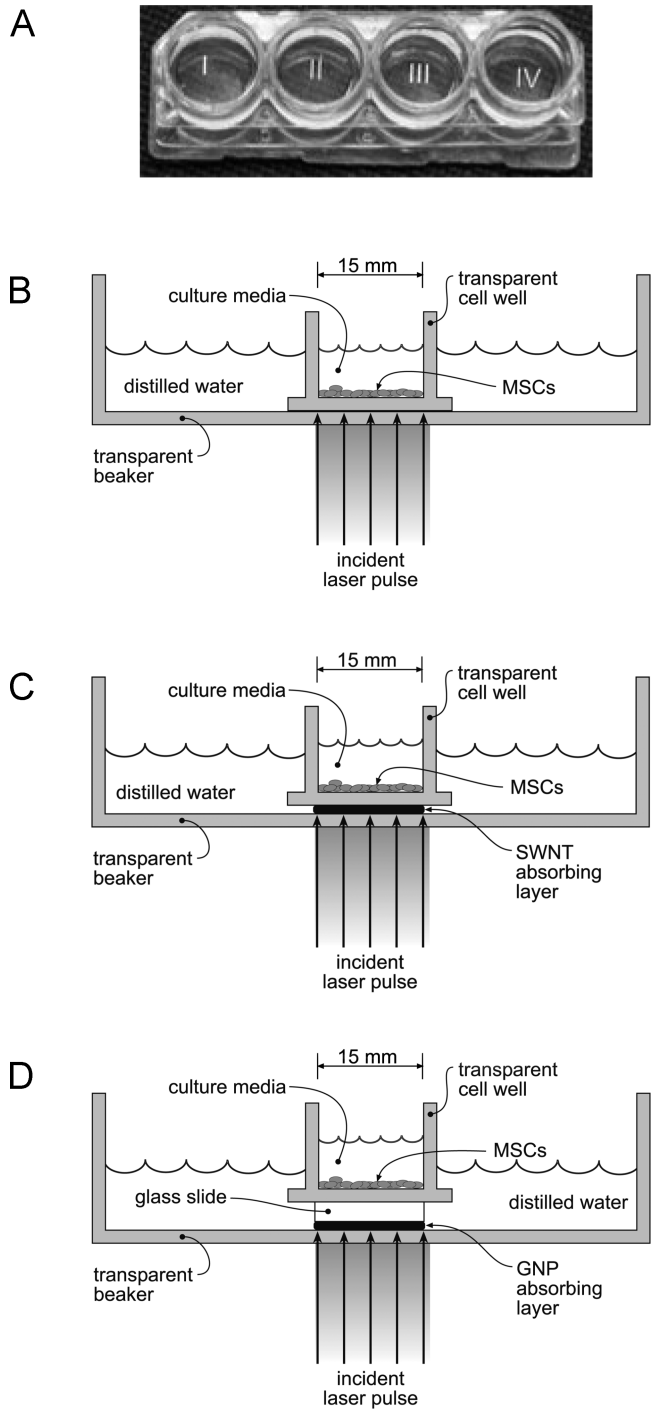

Figure 1. Photoacoustic schematic. (A) Digital image of the Nunc SonicSeal; a 4-well optical-bottom cell culture plate. MSCs incubated in wells II and III were stimulated by the laser, while those incubated in I and IV were not exposed to the laser light and, therefore, experienced only the acoustic effect. (B) Depiction of the PA stimulation setup for the SWNT in media and light groups. The Nunc SonicSeal tissue culture plates were incubated with the MSCs. The tissue culture plate was placed in another (10 cm diameter) polystyrene beaker containing 20 mL of water. The laser beam irradiated the PA groups with a 15 mm beam diameter from below. (C) Depiction of the PA stimulation setup for the SWNT group. SWNTs were completely coated to the outside bottom (underneath) of the 15 mm well, and the laser beam irradiated the PA groups with a 15 mm beam diameter from below. (D) Depiction of the PA stimulation setup for gold groups. GNPs were coated to a glass slide and placed underneath the 15 mm well, and the laser beam irradiated the PA groups with a 15 mm beam diameter from below.

RESULTS AND DISCUSSION

Pulse Laser Stimulation with Nanoparticles. For all of the groups, MSCs (ATCC-CRL12424) were cultured initially at 20 000 cells/well in DMEM (GIBCO) with 10% FBS (Invitrogen) and 1% penicillin/streptomycin (GIBCO) in 4-well optical-bottom (15 mm diameter) SonicSeal tissue culture plates (Nunc, Naperville, IL) (Figure 1A) without the osteogenic supplements (OS; 0.01 M β-glycerophosphate, 50 mg/L ascorbic acid, 10^{-8} M dexamethasone) shown to differentiate MSCs toward osteoblasts.[20,21] Figure 1B–D shows the experimental setup. The tissue culture plates were placed inside a 10 cm polystyrene beaker, filled with 20 mL of water. Water was used because it does not absorb laser light, is transparent, and acts as a coupling medium for acoustic wave propagation.

The center two wells (II, III in Figure 1A) were the only ones directly exposed to the laser during the stimulation. A summary of all the experimental groups is presented in Table 1. Three groups were used as controls: MSCs incubated in media without OS and without PA stimulation (control 1), MSCs incubated in media with SWNTs without OS and without PA stimulation (control 2), and MSCs incubated in media with OS and without PA stimulation (control 3). Four groups were used for the photoacoustic stimulation: MSCs without nanoparticles directly stimulated by the laser (light) (Figure 1B), 10 ppm of SWNTs directly incubated with the MSCs (SWNT in media) (Figure 1B), SWNTs coated to the outside bottom (underneath) of the tissue culture plate (SWNT) (Figure 1C), and GNPs coated onto a glass slide and placed underneath the tissue culture plate (gold) (Figure 1D). The first two groups were used to investigate the effect of PA stimulation on the osteodifferentiation of the MSCs in the presence and absence of nanoparticles in the media. The final two groups (SWNT and gold) were used to investigate the contribution of the acoustic waves generated by the nanoparticles on the differentiation of the MSCs and whether different nanoparticles with good PA properties have similar abilities to facilitate the differentiation of MSCs toward osteoblasts. Additional groups with GNPs were not included because the information obtained was sufficient to provide answers to the following specific questions: (1) Does PA stimulation differentiate MSCs toward osteoblasts? (2) What effect does PA stimulation combined with nanoparticles that enhance the PA effect have on the osteodifferentiation of the MSCs? SWNTs were given more emphasis than GNPs because our recent results suggest that SWNTs generate acoustic signals by absorption of electromagnetic energy in the visible/NIR as well as radio frequency region.[22,23] This characteristic property of the SWNTs would be beneficial for future *in vivo* studies, where one can use a variety of electromagnetic sources for deeper tissue penetration. In both of the groups (SWNT and gold), SWNTs and GNPs underneath the cell culture plates avoided di-

TABLE 1. Summary of Experimental Groups and the Conditions Tested

experimental groups	OS included	nanoparticles included	PA stimulation performed
SWNT in media	no	yes, SWNTs incubated with the cells	yes
gold	no	yes, GNPs coated to the outside bottom (underneath) the tissue culture plate	yes
SWNT	no	yes, SWNTs coated to the outside bottom (underneath) the tissue culture plate	yes
light	no	no	yes
control 1	no	no	no
control 2	no	yes, SWNTs incubated with the cells	no
control 3	yes	no	no

OS = osteogenic supplements; PA = photoacoustic; SWNT = single-walled carbon nanotube; GNP = gold nanoparticles

rect contact with the cells (Figure 1C,D). The incoming laser light was completely absorbed by the nanoparticles with negligible transmittance,[24,25] and the MSCs only felt the generated acoustic waves. Each group was stimulated for 10 min a day using a 527 nm Nd:YLF laser with a 200 ns pulse duration, at a pulse repetition rate of 10 Hz (~6000 pulses/day). The incident laser fluence on the sample surface was controlled to ~6 mJ/cm^2 to be within the American National Standards Institute (ANSI) standard of maximum permissible exposure (MPE). This exposure was repeated for 4, 9, or 16 days. The differentiation of MSCs for the stimulated and the nonstimulated groups was determined by analysis of known indicators for cell proliferation (cellular DNA analysis), osteogenesis (production of alkaline phosphatase (ALP), deposition of a calcified matrix (Ca content analysis), and osteopontin (OPN) expression)), adipogenesis (lipid quantification), and chondrogenesis (sulfated glycosaminoglycan (sGAG) expression).

Cellular Response to Stimulation. It is now well-established that osteodifferentiation is marked by sequential stages of cellular proliferation and bone extracellular matrix maturation.[26] Thus, the cellularity (Figure 2) for each group was quantified as a measure of proliferation by analyzing DNA content using the PicoGreen assay shown to correlate DNA content directly to cell number.[18] The cell numbers of the PA stimulated groups were higher (greater than 17%) than the nonstimulated control 1 after 9 days of irradiation. The general trend observed for the cellularity for the PA stimulated groups was consistent with what is normally observed for this cell type,[18] an increase in cell growth and a growth plateau between day 9 and day 16. The plateau in cellularity between day 9 and day 16 may be due to an increase in matrix deposition and mineralization (Figure 5 and Table S1 in the Supporting Information) with time.[18] The DNA could be encased within the matrix and may not be detectable by the DNA assay. Alternatively, the plateau effect may also be an indication of poor cell proliferation or cell death. However, the extensive mineralization and changes in expression of osteoblastic markers (Figures 3−6) observed in all of the groups suggest that the cells remain viable with continued matrix deposition.

Figure 3 shows the results of ALP activity for all of the groups. ALP activity is a transient early marker of osteodifferentiation in MSCs known to peak at the end of the proliferative stage and before matrix maturation.[27] At each time point, the ALP activity of the stimulated groups was significantly higher (up to ~2050% greater at day 9) than the nonstimulated controls. The nonstimulated groups without OS (controls 1 and 2; data included in Table S2 in the Supporting Information) did not show any noticeable increase in ALP activity or in other markers, indicating that these cells were not differentiating. A general trend in ALP activity during osteodifferentiation is an initial increase with proliferation and a subsequent slowing down with matrix deposition and mineralization.[28] The ALP activity peaked between day 9 and day 16 for the stimulated groups before decreasing by day 16, suggesting that osteodifferentiation was indeed occurring. Furthermore, ALP content for the stimulated SWNT in media, SWNT, and gold groups was greater than the light groups at all time points (up to ~168% greater at day 9).

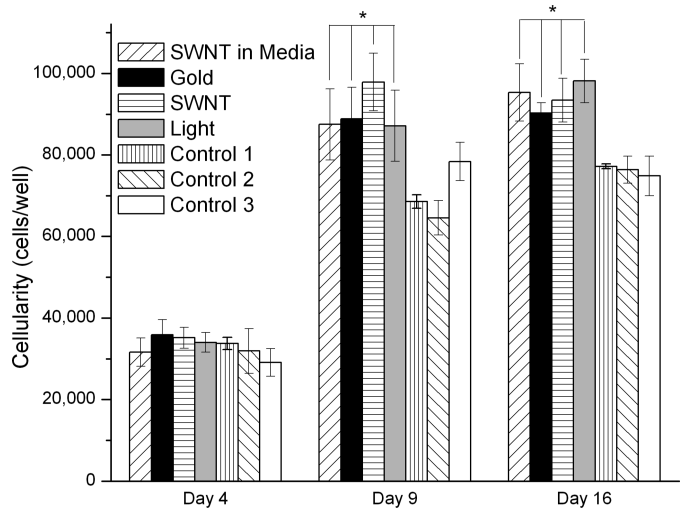

Figure 2. Cellularity of all PA stimulated groups and controls after 4, 9, and 16 days. Experimental groups were 10 ppm of SWNTs directly incubated with the MSCs (SWNT in media), GNPs coated onto a glass slide and placed underneath the tissue culture plate (gold), SWNTs coated to the outside bottom (underneath) of the tissue culture plate (SWNT), MSCs without nanoparticles directly stimulated by the laser (light), MSCs incubated in media without OS and without PA stimulation (control 1), MSCs incubated in media with SWNTs without OS and without PA stimulation (control 2), and MSCs incubated in media with OS and without PA stimulation (control 3). Data represented as mean ± standard deviation for $n = 4$; * represents statistical difference ($P < 0.05$) compared to the nonstimulated control 1.

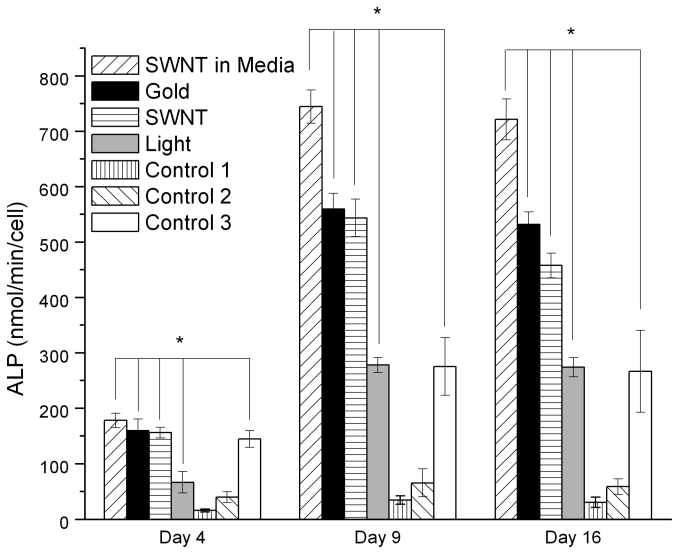

Figure 3. Alkaline (ALP) phosphatase activity of all PA stimulated groups and controls after 4, 9, and 16 days. Experimental groups were 10 ppm of SWNTs directly incubated with the MSCs (SWNT in media), GNPs coated onto a glass slide and placed underneath the tissue culture plate (gold), SWNTs coated to the outside bottom (underneath) of the tissue culture plate (SWNT), MSCs without nanoparticles directly stimulated by the laser (light), MSCs incubated in media without OS and without PA stimulation (control 1), MSCs incubated in media with SWNTs without OS and without PA stimulation (control 2), and MSCs incubated in media with OS and without PA stimulation (control 3). Data represented as mean ± standard deviation for $n = 4$; * represents statistical difference ($P < 0.05$) compared to the nonstimulated control 1.

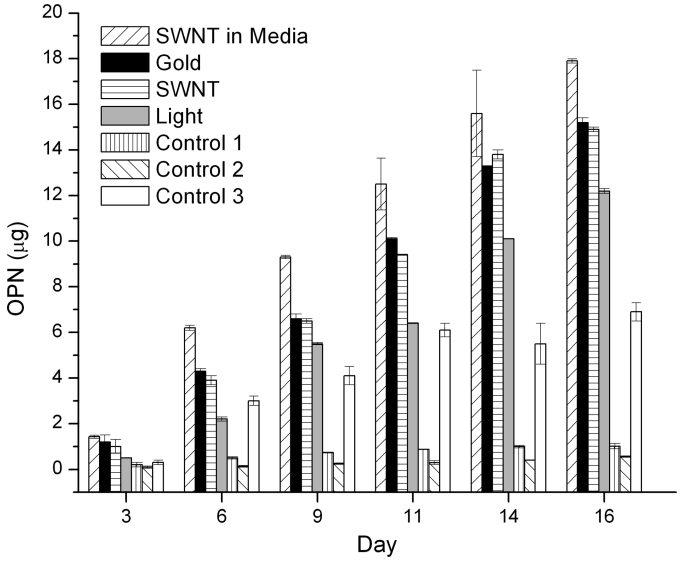

Figure 4. OPN protein expression in the media samples of the PA groups and controls over 16 days. Experimental groups were 10 ppm of SWNTs directly incubated with the MSCs (SWNT in media), GNPs coated onto a glass slide and placed underneath the tissue culture plate (gold), SWNTs coated to the outside bottom (underneath) of the tissue culture plate (SWNT), MSCs without nanoparticles directly stimulated by the laser (light), MSCs incubated in media without OS and without PA stimulation (control 1), MSCs incubated in media with SWNTs without OS and without PA stimulation (control 2), and MSCs incubated in media with OS and without PA stimulation (control 3). Total OPN protein expression in the extracellular media was measured after each media change.

The osteoblastic proliferation of the MSCs is further confirmed by the presence of osteopontin. Osteopontin, a phosphorylated glycoprotein, is an early marker secreted by osteoblasts during early stages of bone development and has been thought to promote cell attachment essential for matrix mineralization.[29] Figure 4 shows the accumulation of secreted osteopontin in the culture media over 16 days. It clearly shows a linear temporal increase in osteopontin for the stimulated groups with negligible detection in the nonstimulated static cultures (control 1). For all PA stimulated groups, there is an increase in osteopontin secretion with time. Since osteopontin is considered a direct indicator of osteoblastic proliferation *in vitro*,[30] the results suggest a continuous osteoblastic proliferation for the duration of the study. The osteopontin levels for SWNT in media > SWNT, gold > light, which implies that proliferation of cells for SWNT in media > SWNT, gold > light even though the cellularity results (Figure 2) were inconclusive with respect to cell proliferation between day 9 and day 16 and only indicate that PA stimulation increases proliferation up to day 9.

The accelerated osteoblastic differentiation for all the PA stimulated groups and the trend of increased proliferation of cells for SWNT in media > SWNT, gold > light discussed above are further corroborated by calcium deposition, a late stage marker of osteoblast differentiation.[18,28] The production and deposition of a calcified, mineralized matrix are considered to be indicators of maturation of osteoblast phenotype for MSCs' differentiation. Thus, the calcium content for all of the groups was quantified to evaluate their matrix production. The calcium content for all of the groups presented in Figure 5 shows that the measured calcium content for the PA stimulated groups increased substantially with the highest values at day 16. Control 1 and control 2 had low detectable calcium (Table S3 in the Supporting Information). The onset of calcium deposition seen at day 4 for the PA stimulated groups is in accordance to the accelerated osteodifferentiation as indicated by the osteopontin data. After 16 days, the SWNT in media group contained 318 μg, SWNT contained 221 μg, gold contained 243 μg, and light contained 161 μg of calcium. In comparison, control 1, control 2, and control 3 yielded 0.16, 0.11, and 45 μg, respectively. Thus, SWNT in media yielded a 612%, SWNTs yielded a 396%, gold yielded a 444%, and light yielded a 260% increase compared to the control 3 (MSCs cultured with OS). Among the PA stimulated groups, at day 16, SWNT in media showed 44 and 97% greater Ca content than SWNT and light, respectively. Gold and SWNT showed 51 and 38% greater Ca content than light, respectively. This trend among the PA stimulated groups for Ca content is similar to the trend of increased osteopontin (Figure 4) with SWNT in media > SWNT, gold > light. Taken together, it is logical to infer the PA stimulated groups show accelerated differentiation and increased cell proliferation.

Chondrogenic and adipogenic assays were also performed for the PA stimulated groups to ascertain the

presence of other major lineages (adipocytes and chondrocytes) after PA stimulation. Chondrogenesis was assessed by quantifying the amount of extracellular proteoglycans, using sulfated glycosaminoglycan (sGAG) as a marker.[31] The groups were also stained with Oil Red O to identify and quantify lipid-containing vacuoles, a good indicator of adipogenesis. At all time points for the PA stimulated groups, the chondrogenic assay showed negligible amounts of sGAG (Table S4 in the Supporting Information), and no Oil Red O staining was observed, indicating that the MSCs did not differentiate toward chondrocytes and adipocytes.

As mentioned earlier, the two groups, SWNT and gold, were used to investigate the contribution of the acoustic waves generated by the nanoparticles on the differentiation of the MSCs. Figure 6 shows the Ca content at day 16 for SWNT, gold, and light directly exposed to the laser (wells II and III in Figure 1A) and the Ca content of adjacent wells (I and IV in Figure 1A), which only experienced the acoustic waves. No statistically significant difference in the Ca content was observed for wells directly in the pathway of the laser light or the adjacent wells. These results indicate that for SWNT, gold, and light the observed effect is mainly due to the acoustic waves. However, the greater Ca content for SWNT (~221 μg) compared to light (~161 μg) suggests that the acoustic waves generated by SWNTs have a greater beneficial effect on the cells. Combining the two, we hypothesize that for SWNT in media, which has the highest Ca content compared to other groups, the generated acoustic waves play a dominant stimulatory role.

There is now a body of work investigating the effects of optical and ultrasound stimulation on osteogenesis.[32,33] Optical stimulation efficacy is affected by the laser system (*e.g.*, He−Ne, semiconductor, *etc.*), the specifications of the optical source (*e.g.*, wavelength, output power, *etc.*), and the optical wave type (*e.g.*, continuous, interrupted, pulsed).[32,34,35] The mechanism of osteoinduction by laser stimulation, though not completely clear, has been thought to be photochemical in nature, with the intracellular mitochondrial chromophores absorbing the incident photons and enhancing cell proliferation.[35,36] For ultrasound, its efficacy for osteoinduction is affected by the specific characteristics of the ultrasound signal (*e.g.*, frequency, pulse width, *etc.*).[33] The mechanism of ultrasound stimulation has been attributed to the acoustic pressure waves or mechanical signals generated by the ultrasound. These mechanisms have been suggested to induce conformational and biochemical changes to the cell membrane leading to downstream alterations in bone-specific genes.[33] Analysis of our results (as discussed above) indicates that, for both the SWNT in media group and the light group, the mechanism of osteoinduction may be a combination of photochemical and mechanical signals with the mechanical contributions playing a dominant role, while for SWNT and gold, the mechanism is only due to mechanical contributions. It is important to point out here that these PA mechanical signals are unlike the ones used in ultrasound stimulation. For ultrasound stimulation, sine waves of a certain ultrasound frequency (typically in megahertz) are used. For PA stimulation, the acoustic

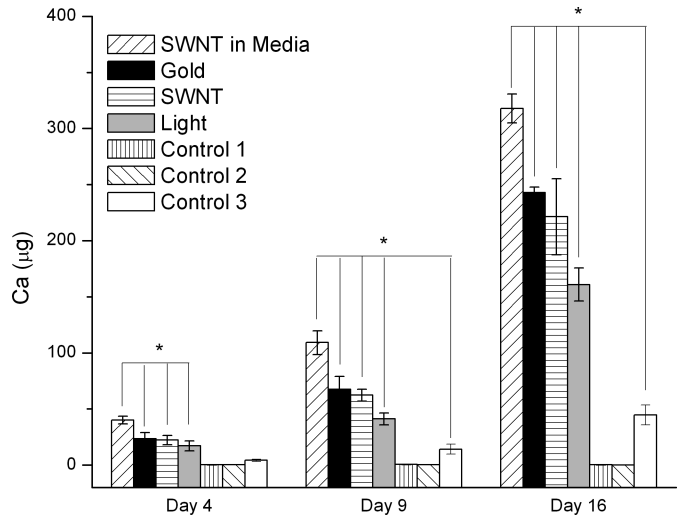

Figure 5. Calcium content of all the groups after 4, 9, and 16 days. Note that the calcium content for control 1 and control 2 was negligible compared to the other groups, and hence, the *y*-axis starts at a value slightly lower than zero so that they show up on the graph. Experimental groups were 10 ppm of SWNTs directly incubated with the MSCs (SWNT in media), GNPs coated onto a glass slide and placed underneath the tissue culture plate (gold), SWNTs coated to the outside bottom (underneath) of the tissue culture plate (SWNT), MSCs without nanoparticles directly stimulated by the laser (light), MSCs incubated in media without OS and without PA stimulation (control 1), MSCs incubated in media with SWNTs without OS and without PA stimulation (control 2), and MSCs incubated in media with OS and without PA stimulation (control 3). Data represented as mean ± standard deviation for $n = 4$; * represents statistical difference ($P < 0.05$) compared to the nonstimulated control 1.

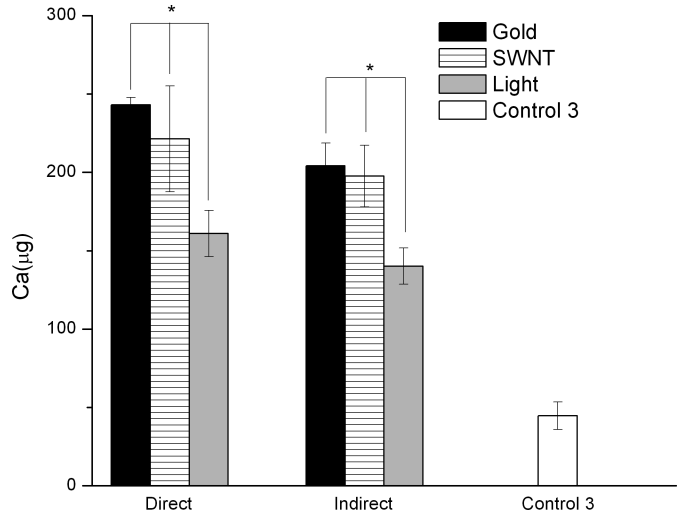

Figure 6. Calcium content after 16 days for the PA groups and control 3. The direct samples were in the path of the laser light during PA stimulation. The indirect samples were the adjacent wells not in the path of the laser light. Data represented as mean ± standard deviation for $n = 4$; * represents statistical difference ($P < 0.05$) between the PA groups and the nonstimulated control 3.

waves generated span a whole range of frequencies from kilohertz to megahertz. To further elucidate the mechanism, intensive studies are currently underway in our lab.

Recently, a number of studies have shown that the SWNTs and GNPs facilitate thermal ablation of cells under continuous laser irradiation.[37−40] Our results in conjugation with these studies show that the same nanoparticles under different laser conditions can either regenerate or destroy cells and tissues.

The demonstration of the nanoparticles to facilitate and promote osteogenesis under PA stimulation introduces a new paradigm for bone regeneration applications especially at near-infrared (NIR) and radio frequency (rf) domains of the electromagnetic spectrum, which allows deeper tissue penetration, and where these nanoparticles have shown to have good absorptive and PA properties.[23,41] For example, in bone tissue engineering, most porous scaffolds (*e.g.*, ceramics,[42] metals,[43] polymers,[44] and nano-reinforced)[45] are only osteoconductive (promoting bone ingrowth). To incorporate osteoinductive properties into scaffolds, strategies include incorporating (covalently or noncovalently) peptides, nanosized hydroxyapitite,[46] growth factors,[46] and cytokines specifically known to influence bone cells and performing scaffold surface treatments.[47] Incorporation of nanoparticles used in this study into tissue engineering scaffolds and the PA stimulation of these scaffolds should introduce a novel biophysical rather than biochemical strategy to induce osteoinductive properties. Another example is in osteoporosis, where the nanoparticles can be functionalized with antiresorptive drugs (*e.g.*, bisphosphonates), allowing a multi-prong pharmacological and nonpharmacological (PA stimulation) strategy that would slow down bone loss due to the drugs, while simultaneously allowing high-sensitivity, deep-tissue, and targeted regeneration of bone due to nanoparticle-facilitated PA stimulation.

CONCLUSION

In summary, we report the osteodifferentiation of MSCs by a novel nanoparticle-enhanced biophysical technique. We show that a brief (10 min) daily nanosecond pulse laser-induced PA stimulation enhanced by nanoparticles (SWNTs and GNPs), over 16 days, facilitates MSCs' differentiation toward osteoblasts. The PA stimulated groups, after 16 days, show increased calcium deposition (up to 612% increase) and osteopontin levels compared to the controls cultured with osteogenic supplements (without PA stimulation). Among the PA stimulated groups, at day 16, the groups with nanoparticles show increased calcium deposition (up to 97% greater) than those that did not contain nanoparticles. The results demonstrate that PA stimulation not only promotes osteogenesis but also is synergistically enhanced by the presence of nanoparticles and, thus, may have major implications for bone regeneration applications.

EXPERIMENTAL METHODS

Cell Culture. Mouse marrow stromal cells (MSCs; ATCC-CRL12424) were cultured in DMEM (GIBCO) with 10% FBS (Invitrogen) and 1% penicillin/streptomycin (GIBCO). Cells grown in osteogenic supplemented media also contained 10^{-8} M dexamethasone (Sigma), 10 mM β-glycerophosphate (Sigma), and 5 μg/mL L-ascorbic acid (Sigma). MSCs were initially plated onto optical bottom SonicSeal Slide Wells (Nunc) at 20 000 cells/well. Culture medium was changed every 2−3 days and replenished with 0.5 mL of fresh medium. The aspirated medium was stored at 4 °C for later osteopontin quantification. After stimulation, medium was removed from the samples and 1 mL of DI water was added to each well and frozen at −20 °C for the osteoblast proliferation assays. The tissue culture plates were kept under standard cell culture conditions: 37 °C, 95% relative humidity, and 5% CO_2/95% air environment.

Photoacoustic Setup. A 527 nm (green light) Nd:YLF short pulse laser (Photonics Industries GM-30) produced laser pulses with a pulse duration of ∼200 ns and a pulse energy of 10 mJ at a repetition rate of 10 Hz directly under each SonicSeal tissue culture well (15 mm diameter) containing MSCs for 10 min daily for 4, 9, or 16 consecutive days. The 10 min stimulation time was chosen based on previous optical and ultrasound stimulation work reported in literature.[32−36] The stimulation was performed under nominal laboratory conditions (25 °C, 1 atm). During stimulation, these wells were placed into a 10 cm polystyrene beaker containing 20 mL of water. The group SWNT had ∼2 mg of SWNTs (1.2−1.5 nm diameter, 2−5 μm length) (Sigma Aldrich, 519308) secured using superglue (Elmer's Products, Columbus, OH) to the outside bottom of the tissue culture wells. The glue was colorless and transparent to the laser light. The group gold had ∼2 mg of gold nanoparticles coated onto a 1 mm quartz glass slide through a previously described deposition method,[48] and it was then placed below the tissue culture well. For the deposition of the GNPs, a gold pellet (Kurt Lesker-EVMAUXX40G, Pittsburgh, PA) was placed into a crucible (Alfa Aesar, Ward Hill, MA), and the glass slide was taped to a 4 in. silicon wafer and placed into a vacuum chamber under pressure ($<2 \times 10^{-6}$ Torr) at 300 °C, with a deposition rate of 30 nm/s. The gold was vaporized and coated onto the glass surface, with ∼130 nm gold thickness, and then annealed for 18 h at 300 °C to form closely packed GNPs of size 50−80 nm. Gold could not be coated directly onto the cell culture plate due to the high temperatures which would have melted the plate. The procedures used to coat the SWNTs and GNPs also allowed formation of good uniform adherent films. The group SWNT in media had 10 ppm of SWNTs directly incubated with the MSCs. This concentration was chosen based on our previous work, which showed that incubation at these low dosages does not affect the viability of the MSCs.[45] The control samples were not exposed to the laser. All groups had a sample size of $n = 4$. Before the experiment began on the PA groups, a needle hydrophone transducer (Precision Acoustics) connected to an oscilloscope (GW Instek) was used to confirm an acoustic signal.

Cellularity Assay. The cellularity of all the groups were determined by quantifying the DNA content of the lysated cells using a fluorometric DNA quantification kit (Picogreen Elisa kit, Invitrogen, Carlsbad, CA) with results expressed as cells by quantifying the DNA content of a known amount of MSCs.[18] Briefly, samples were sonicated for 5 min to lyse the cells to allow cellular DNA into the solution. In a separate 96-well plate, the buffer provided with the kit was added to each well of a 96-well plate at 100 μL/well, and 100 μL of standards and samples was added in triplicate. Then 100 μL of Picogreen reagent was added to each well and allowed to incubate at room temperature for 10 min in a dark room. The fluorescence of each well was

measured using a microplate reader (Biotek, Winooski, VT) at a 480 nm excitation and 520 nm emission wavelength. The cell number for each group was determined by correlating measured DNA amount with a known number of MSCs, which was 3.11 pg of DNA per cell.

Calcium Assay. Calcium content is a later stage marker of osteogenesis and is quantified to determine the formation of a calcified extracellular matrix. Calcium quantification was performed by adding 1 M acetic acid to an equal volume of cellular sample and put on a shaker overnight to dissolve the Ca.[18] Calcium chloride (Sigma) was used as the standard. For the assay, 20 μL of samples or standard was added in triplicate into each well of a 96-well plate. To each well, 280 μL of Arsenazo III calcium assay reagent (Diagnostic Chemicals, Oxford, CT) was then added. This reagent is a calcium binding chelate and changes color upon chelating dissolved calcium, and this color change corresponds to calcium ion concentration. Absorbance was determined at 650 nm on a microplate reader.

Alkaline Phosphatase Assay. Alkaline phosphatase activity is an early stage marker of osteogenesis. Alkaline phosphatase was quantified by the following method:[18] 100 μL of *p*-nitrophenyl phosphate (pNPP) liquid substrate system (Sigma) was added to 100 μL of sample or standard in triplicate and incubated for 1 h at 37 °C in a 96-well cell plate. pNPP is hydrolyzed by the alkaline phosphatase forming *p*-nitrophenol; 100 μL of 0.2 M NaOH was added to stop the reaction. The absorbance was read at 405 nm on a microplate reader (Biotek, Winooski, VT), and alkaline phosphatase activity was quantified by comparison to the 4-nitrophenol (Sigma) standards.

Osteopontin Assay. Osteopontin (OPN), similar to calcium, is a late stage marker of osteogenesis and is secreted from osteoblasts into the extracellular media. To quantify OPN, the mouse OPN Elisa kit (R&D Systems, Minneapolis, MN) was used. Sample culture media was collected every 2−3 days and was diluted 10 000-fold in DMEM, and the assay was performed in duplicate. Briefly, 50 μL of assay diluent and 50 μL of standard or samples were added to wells that were precoated with an OPN polyclonal antibody allowing the OPN to bind and incubated for 2 h at room temperature. Then the samples and standards were aspirated, and 100 μL of an enzyme-linked polyclonal antibody reagent was added to each well and incubated at room temperature for 2 h and followed by aspiration; 100 μL of substrate solution was added to the wells for 30 min in the dark, causing a blue color when an enzyme reaction occurred, and the reaction was stopped with 100 μL of hydrochloric acid turning the samples yellow. Absorbance was determined at 450 nm on a microplate reader, and OPN level was determined by the comparison to the OPN mouse standards.

Sulfated Glycosaminoglycan Assay. Sulfated glycosaminoglycan content was analyzed as a marker for chondrogenesis because these proteoglycans are released from chondrocytes.[49] To determine the level of chondrogenesis, sulfated glycosaminoglycan content was quantified using 1,9-dimethyl methylene blue solution (DMB; 40 mM NaCl, 40 mM glycine, 46 μM DMB (Sigma-Aldrich) in PBE buffer (100 mM phosphate, 5 mM EDTA; pH = 7.5)), with pH adjusted to 3.0 was used as the reagent.[49] DMB solution (250 μL) was added to 20 μL of sample culture media or standard in triplicate. The standards were chondroitin sulfate (Sigma) dissolved in PBE buffer. Absorbance was read on a plate reader at 525 nm.

Oil Red O Assay. Oil Red O was used as a stain on the groups to identify and quantify lipid-containing vacuoles, which are considered good indicators of adipogenesis. For adipogenic qualitative and quantitative analysis,[50] the cells were washed with PBS and fixed in 10% formalin for 1 h and rinsed with water. The cells were stained with Oil Red O (Sigma) for 15 min (6 parts Oil Red O (0.6% Oil Red O in isopropanol) and 4 parts water) and washed with 70% ethanol and water. To quantify, 200 μL of 4% IGEPAL Ca-630 (Sigma) in isopropanol was added to the cells for 5 min and was transferred to a 96-well plate in triplicate to read absorbance at 520 nm on a plate reader.

Statistical Analysis. The ALP, DNA, calcium, sGAG, and adipogenesis assays were done in triplicate, and the OPN assay was done in duplicate. Statistical analysis was done using a one-way ANOVA. The data are represented in means ± standard deviation for $n = 4$. Tukey's "Honestly Significantly Different" (HSD) multiple comparison test was used to determine the effects of the parameters examined. All comparisons were conducted at a 95% confidence interval ($P < 0.05$).

Acknowledgment. The authors thank P. Uppal, J. Jerome, Y.X. Qin, J. Cheng, and A. Kadam for their experimental assistance. This research was supported by the Office of the Vice President of Research at Stony Brook University (SB).

Supporting Information Available: Tables S1−S4. This material is available free of charge *via* the Internet at http://pubs.acs.org.

REFERENCES AND NOTES

1. Bell, A. G. On the Production and Reproduction of Sound by Light. *Am. J. Sci.* **1880**, 305–324.
2. McDonald, F. A. Photoacoustic Effect and the Physics of Waves. *Am. J. Phys.* **1980**, *48*, 41–47.
3. Xu, M.; Wang, L. V. Photoacoustic Imaging in Biomedicine. *Rev. Sci. Instrum.* **2006**, *77*, 041101–041122.
4. Zerda, A. D. L.; Zavaleta, C.; Keren, S.; Vaithilingam, S.; Bodapati, S.; Liu, Z.; Levi, J.; Smith, B. R.; Ma, T.-J.; Oralkan, O.; *et al.* Carbon Nanotubes as Photoacoustic Molecular Imaging Agents in Living Mice. *Nat. Nanotechnol.* **2008**, *3*, 557–562.
5. Yang, X.; Skrabalak, S. E.; Li, Z. Y.; Xia, Y.; Wang, L. V. Photoacoustic Tomography of a Rat Cerebral Cortex *In Vivo* with Au Nanocages as an Optical Contrast Agent. *Nano Lett.* **2007**, *7*, 3798–3802.
6. Eghtedari, M.; Oraevsky, A.; Copland, J. A.; Kotov, N. A.; Conjusteau, A.; Motamedi, M. High Sensitivity of *In Vivo* Detection of Gold Nanorods Using a Laser Optoacoustic Imaging System. *Nano Lett.* **2007**, *7*, 1914–1918.
7. Tondreau, T.; Lagneaux, L.; Dejeneffe, M.; Massy, M.; Mortier, C.; Delforge, A.; Bron, D. Bone Marrow-Derived Mesenchymal Stem Cells Already Express Specific Neural Proteins before Any Differentiation. *Differentiation* **2004**, *72*, 319–326.
8. Pittenger, M. F.; Mackay, A. M.; Beck, S. C.; Jaiswal, R. K.; Douglas, R.; Mosca, J. D.; Moorman, M. A.; Simonetti, D. W.; Craig, S.; Marshak, D. R. Multilineage Potential of Adult Human Mesenchymal Stem Cells. *Science* **1999**, *284*, 143–147.
9. Caplan, A. I. Review: Mesenchymal Stem Cells: Cell Based Reconstructive Therapy in Orthopedics. *Tissue Eng.* **2005**, *11*, 1198–1211.
10. Caplan, A. I. Adult Mesenchymal Stem Cells for Tissue Engineering *versus* Regenerative Medicine. *J. Cell. Physiol.* **2007**, *213*, 341–347.
11. Mikos, A. G.; Herring, S. W.; Ochareon, P.; Elisseeff, J.; Lu, H. H.; Kandel, R.; Schoen, F. J.; Toner, M.; Mooney, D.; Atala, A.; *et al.* Engineering Complex Tissues. *Tissue Eng.* **2006**, *12*, 3307–3339.
12. Prockop, D. J. Marrow Stromal Cells as Stem Cells for Continual Renewal of Nonhematopoietic Tissues and as Potential Vectors for Gene Therapy. *J. Cell. Biochem.* **1998**, *72*, 284–285.
13. Clinicaltrails.gov, a Service of the U.S. National Institues of Health.
14. Abramovitch-Gottlib, L.; Gross, T.; Naveh, D.; Geresh, S.; Rosenwaks, S.; Bar, I.; Vago, R. Low Level Laser Irradiation Stimulates Osteogenic Phenotype of Mesenchymal Stem Cells Seeded on a Three-Dimensional Biomatrix. *Lasers Med. Sci.* **2005**, *20*, 138–146.
15. Kim, H.; Kim, J.; Abbas, A.; Kim, D.-O.; Park, S.-J.; Chung, J.; Song, E.; Yoon, T. Red Light of 647 nm Enhances Osteogenic Differentiation in Mesenchymal Stem Cells. *Lasers Med. Sci.* **2009**, *24*, 214−222.
16. Naruse, K.; Miyauchi, A.; Itoman, M.; Mikuni-Takagaki, Y. Distinct Anabolic Response of Osteoblast to Low-Intensity Pulsed Ultrasound. *J. Bone Miner. Res.* **2003**, *18*, 360–369.
17. Li, Y. J.; Batra, N. N.; You, L.; Meier, S. C.; Coe, I. A.; Yellowley, C. E.; Jacobs, C. R. Oscillatory Fluid Flow Affects Human Marrow Stromal Cell Proliferation and Differentiation. *J. Orthop. Res.* **2004**, *22*, 1283–1289.
18. Datta, N.; Holtorf, H. L.; Sikavitsas, V. I.; Jansen, J. A.; Mikos,

A. G. Effect of Bone Extracellular Matrix Synthesized *In Vitro* on the Osteoblastic Differentiation of Marrow Stromal Cells. *Biomaterials* **2005**, *26*, 971–977.
19. Lee, K.-W.; Wang, S.; Yaszemski, M. J.; Lu, L. Physical Properties and Cellular Responses to Crosslinkable Poly(propylene fumarate)/Hydroxyapatite Nanocomposites. *Biomaterials* **2008**, *29*, 2839–2848.
20. Porter, R. M.; Huckle, W. R.; Goldstein, A. S. Effect of Dexamethasone Withdrawal on Osteoblastic Differentiation of Bone Marrow Stromal Cells. *J. Cell. Biochem.* **2003**, *90*, 13–22.
21. Peter, S. J.; Liang, C. R.; Kim, D. J.; Widmer, M. S.; Mikos, A. G. Osteoblastic Phenotype of Rat Marrow Stromal Cells Cultured in the Presence of Dexamethasone, β-Glycerolphosphate, and L-Ascorbic Acid. *J. Cell. Biochem.* **1998**, *71*, 55–62.
22. Pramanik, M.; Song, K. H.; Swierczewska, M.; Green, D.; Sitharaman, B.; Wang, L. H. V. *In Vivo* Carbon Nanotube-Enhanced Non-invasive Photoacoustic Mapping of the Sentinel Lymph Node. *Phys. Med. Biol.* **2009**, *54*, 3291–3301.
23. Pramanik, M.; Swierczewska, M.; Green, D.; Sitharaman, B.; Wang, L. V. Single-Walled Carbon Nanotubes as a Multimodal-Thermoacoustic and Photoacoustic-Contrast Agent. *J. Biomed. Opt.* **2009**, *14*, 034018.
24. Zhu, J.; Li, J.-J.; Zhao, J.-W.; Bai, S.-W. Light Absorption Efficiencies of Gold Nanoellipsoid at Different Resonance Frequency. *J. Mater. Sci.* **2008**, *43*, 5199–5205.
25. Yang, Z.-P.; Ci, L.; Bur, J. A.; Lin, S.-Y.; Ajayan, P. M. Experimental Observation of an Extremely Dark Material Made by a Low-Density Nanotube Array. *Nano Lett.* **2008**, *8*, 446–451.
26. Quarles, L. D.; Yohay, D. A.; Lever, L. W.; Caton, R.; Wenstrup, R. J. Distincy Proliferative and Differentiated Stages of Murine Mc3t3-E1 Cells in Culture: An *In Vitro* Model of Osteoblast Development. *J. Bone Miner. Res.* **1992**, *7*, 683–692.
27. Owen, T. A.; Aronow, M.; Shalhoub, V.; Barone, L. M.; Wilming, L.; Tassinari, M. S.; Kennedy, M. B.; Pockwinse, S.; Lian, J. B.; Stein, G. S. Progressive Development of the Rat Osteoblast Phenotype *In Vitro*: Reciprocal Relationships in Expression of Genes Associated with Osteoblast Proliferation and Differentiation During Formation of the Bone Extracellular Matrix. *J. Cell. Physiol.* **1990**, *143*, 420–430.
28. Lian, J. B.; Stein, G. S. Concepts of Osteoblast Growth and Differentiation: Basis for Modulation of Bone Cell Development and Tissue Formation. *Crit. Rev. Oral Biol. Med.* **1992**, *3*, 269–305.
29. Mark, M. P.; Butler, W. T.; Prince, C. W.; Finkelman, R. D.; Ruch, J.-V. Developmental Expression of 44-kDa Bone Phosphoprotein (Osteopontin) and Bone Γ-Carboxyglutamic Acid (Gla)-Containing Protein (Osteocalcin) in Calcifying Tissues of Rat. *Differentiation* **1988**, *37*, 123–136.
30. Yamate, T.; Mocharla, H.; Taguchi, Y.; Igietseme, J. U.; Manolagas, S. C.; Abe, E. Osteopontin Expression by Osteoclast and Osteoblast Progenitors in the Murine Bone Marrow: Demonstration of Its Requirement for Osteoclastogenesis and Its Increase after Ovariectomy. *Endocrinology* **1997**, *138*, 3047–3055.
31. Awad, H. A.; Quinn Wickham, M.; Leddy, H. A.; Gimble, J. M.; Guilak, F. Chondrogenic Differentiation of Adipose-Derived Adult Stem Cells in Agarose, Alginate, and Gelatin Scaffolds. *Biomaterials* **2004**, *25*, 3211–3222.
32. Stein, A.; Benayahu, D.; Maltz, L.; Oron, U. Low-Level Laser Irradiation Promotes Proliferation and Differentiation of Human Osteoblasts *In Vitro*. *Photomed. Laser Surg.* **2005**, *23*, 161–166.
33. Rubin, C.; Bolander, M.; Ryaby, J. P.; Hadjiargyrou, M. The Use of Low-Intensity Ultrasound to Accelerate the Healing of Fractures. *J. Bone Joint Surg. Am.* **2001**, *83*, 259–270.
34. Sato, S.; Ogura, M.; Ishihara, M.; Kawauchi, S.; Arai, T.; Matsui, T.; Kurita, A.; Obara, M.; Kikuchi, M.; Ashida, H. Nanosecond, High-Intensity Pulsed Laser Ablation of Myocardium Tissue at the Ultraviolet, Visible, and Near-Infrared Wavelengths: *In-Vitro* Study. *Laser Surg. Med.* **2001**, *29*, 464–473.
35. Luger, E. J.; Rochkind, S.; Wollman, Y.; Kogan, G.; Dekel, S. Effect of Low-Power Laser Irradiation on the Mechanical Properties of Bone Fracture Healing in Rats. *Laser Surg. Med.* **1998**, *22*, 97–102.
36. Friedmann, H.; Lubart, R.; Laulicht, I.; Rochkind, S. A Possible Explanation of Laser-Induced Stimulation and Damage of Cell Cultures. *J. Photochem. Photobiol., B* **1991**, *11*, 87–91.
37. Kam, N. W. S.; O'Connell, M.; Wisdom, J. A.; Dai, H. Carbon Nanotubes as Multifunctional Biological Transporters and Near-Infrared Agents for Selective Cancer Cell Destruction. *Proc. Natl. Acad. Sci. U.S.A.* **2005**, *102*, 11600–11605.
38. Chakravarty, P.; Marches, R.; Zimmerman, N. S.; Swafford, A. D. E.; Bajaj, P.; Musselman, I. H.; Pantano, P.; Draper, R. K.; Vitetta, E. S. Thermal Ablation of Tumor Cells with Antibody-Functionalized Single-Walled Carbon Nanotubes. *Proc. Natl. Acad. Sci. U.S.A.* **2008**, *105*, 8697–8702.
39. Hirsch, L. R.; Stafford, R. J.; Bankson, J. A.; Sershen, S. R.; Rivera, B.; Price, R. E.; Hazle, J. D.; Halas, N. J.; West, J. L. Nanoshell-Mediated Near-Infrared Thermal Therapy of Tumors under Magnetic Resonance Guidance. *Proc. Natl. Acad. Sci. U.S.A.* **2003**, *100*, 13549–13554.
40. O'Neal, D. P.; Hirsch, L. R.; Halas, N. J.; Payne, J. D.; West, J. L. Photo-Thermal Tumor Ablation in Mice Using Near Infrared-Absorbing Nanoparticles. *Cancer Lett.* **2004**, *209*, 171–176.
41. De La Zerda, A.; Zavaleta, C.; Keren, S.; Vaithilingam, S.; Bodapati, S.; Liu, Z.; Levi, J.; Smith, B. R.; Ma, T.-J.; Oralkan, O.; Cheng, Z.; Chen, X.; Dai, H.; Khuri-Yakub, B. T.; Gambhir, S. S. Carbon Nanotubes as Photoacoustic Molecular Imaging Agents in Living Mice. *Nat. Nano* **2008**, *3*, 557–562.
42. Knabe, C.; Driessens, F. C. M.; Planell, J. A.; Gildenhaar, R.; Berger, G.; Reif, D.; Fitzner, R.; Radlanski, R. J.; Gross, U. Evaluation of Calcium Phosphates and Experimental Calcium Phosphate Bone Cements Using Osteogenic Cultures. *J. Biomed. Mater. Res.* **2000**, *52*, 498–508.
43. van den Dolder, J.; Vehof, J. W. M.; Spauwen, P. H. M.; Jansen, J. A. Bone Formation by Rat Bone Marrow Cells Cultured on Titanium Fiber Mesh: Effect of *In Vitro* Culture Time. *J. Biomed. Mater. Res.* **2002**, *62*, 350–358.
44. Fisher, J. P.; Vehof, J. W. M.; Dean, D.; van der Waerden, J. P. C. M.; Holland, T. A.; Mikos, A. G.; Jansen, J. A. Soft and Hard Tissue Response to Photocrosslinked Poly(propylene fumarate) Scaffolds in a Rabbit Model. *J. Biomed. Mater. Res.* **2002**, *59*, 547–556.
45. Sitharaman, B.; Shi, X.; Walboomers, X. F.; Liao, H.; Cuijpers, V.; Wilson, L. J.; Mikos, A. G.; Jansen, J. A. *In Vivo* Biocompatibility of Ultra-Short Single-Walled Carbon Nanotube/Biodegradable Polymer Nanocomposites for Bone Tissue Engineering. *Bone* **2008**, *43*, 362–370.
46. Balasundaram, G.; Sato, M.; Webster, T. J. Using Hydroxyapatite Nanoparticles and Decreased Crystallinity to Promote Osteoblast Adhesion Similar to Functionalizing with Rgd. *Biomaterials* **2006**, *27*, 2798–2805.
47. Hench, L. L.; Polak, J. M. Third-Generation Biomedical Materials. *Science* **2002**, *295*, 1014–1017.
48. Kang, J. F.; Ulman, A.; Liao, S.; Jordan, R.; Yang, G.; Liu, G.-y. Self-Assembled Rigid Monolayers of 4′-Substituted-4-Mercaptobiphenyls on Gold and Silver Surfaces. *Langmuir* **2001**, *17*, 95–106.
49. Farndale, R.; Buttle, D.; Barrett, A. Improved Quantitation and Discrimination of Sulphated Glycosaminoglycans by Use of Dimethylmethylene Blue. *Biochim. Biophys. Acta* **1986**, *883*, 173–177.
50. Kasturi, R.; Joshi, V. C. Hormonal Regulation of Stearoyl Coenzyme a Desaturase Activity and Lipogenesis During Adipose Conversion of 3t3-L1 Cells. *J. Biol. Chem.* **1982**, *257*, 12224–12230.